Cellular Microbiology (2015) **17**(7), 1021–1036
doi:10.1111/cmi.12418
First published online 16 February 2015

Integrin binding by *Borrelia burgdorferi* P66 facilitates dissemination but is not required for infectivity

Laura C. Ristow,[1,2†] Mari Bonde,[3] Yi-Pin Lin,[4] Hiromi Sato,[2,5] Michael Curtis,[1,2] Erin Wesley,[1] Beth L. Hahn,[2,6] Juan Fang,[7] David A. Wilcox,[7] John M. Leong,[4] Sven Bergström[3] and Jenifer Coburn[1,2,6*]

[1]*Graduate Program in Microbiology, Immunology, and Molecular Genetics, Medical College of Wisconsin, Milwaukee, WI, USA.*
[2]*Center for Infectious Disease Research, Medical College of Wisconsin, Milwaukee, WI, USA.*
[3]*Department of Molecular Biology, Umeå University, Umeå, Sweden.*
[4]*Department of Molecular Biology and Microbiology, Tufts University School of Medicine, Boston, MA, USA.*
[5]*Department of Microbiology and Molecular Genetics, Medical College of Wisconsin, Milwaukee, WI, USA.*
[6]*Division of Infectious Diseases, Department of Medicine, Medical College of Wisconsin, Milwaukee, WI, USA.*
[7]*Department of Pediatrics, MACC Fund Research Center, Children's Research Institute, Children's Hospital of Wisconsin and Medical College of Wisconsin, Milwaukee, WI, USA.*

Summary

P66, a *Borrelia burgdorferi* surface protein with porin and integrin-binding activities, is essential for murine infection. The role of P66 integrin-binding activity in *B. burgdorferi* infection was investigated and found to affect transendothelial migration. The role of integrin binding, specifically, was tested by mutation of two amino acids (D205A,D207A) or deletion of seven amino acids (Del202–208). Neither change affected surface localization or channel-forming activity of P66, but both significantly reduced binding to $\alpha_v\beta_3$. Integrin-binding deficient *B. burgdorferi* strains caused disseminated infection in mice at 4 weeks post-subcutaneous inoculation, but bacterial burdens were significantly reduced in some tissues. Following intravenous inoculation, the Del202–208 bacteria were below the limit of detection in all tissues assessed at 2 weeks post-inoculation, but bacterial burdens recovered to wild-type levels at 4 weeks post-inoculation. The delay in tissue colonization correlated with reduced migration of the Del202–208 strains across microvascular endothelial cells, similar to *Δp66* bacteria. These results indicate that integrin binding by P66 is important to efficient dissemination of *B. burgdorferi*, which is critical to its ability to cause disease manifestations in incidental hosts and to its maintenance in the enzootic cycle.

Introduction

Borrelia burgdorferi, the causative agent of Lyme disease, routinely causes disseminated infection in immunocompetent hosts. Dissemination of *B. burgdorferi* throughout the host has long been thought to involve entry into the vasculature near the site of the tick bite and exit from the vasculature in distant tissues, and for brief periods bacteria can be found in the bloodstream. Three types of interactions within the microvasculature, designated tethering, dragging and stationary interactions, have been identified and modelled (Norman *et al.*, 2008; Moriarty *et al.*, 2012). Tethering interactions are brief contacts between the spirochete and the lumen of the vessel, taking less than 1 s to traverse 100 μm along the vessel wall, whereas dragging interactions are defined as a longer contact, 3–20 s to traverse 100 μm along the vessel wall, with the length of the spirochete generally contacting the vessel wall (Norman *et al.*, 2008; Moriarty *et al.*, 2012). Stationary adhesions typically occur at endothelial cell junctions and are thought to be required for eventual transmigration of the spirochete into the surrounding tissue (Norman *et al.*, 2008; Moriarty *et al.*, 2012). An outer surface protein of *B. burgdorferi*, BBK32, possesses two distinct adhesin functions that have been demonstrated to be involved in two distinct types of vascular interactions. BBK32-fibronectin binding is required for tethering interactions and BBK32-glycosaminoglycan (GAG) binding is involved in dragging interactions (Moriarty *et al.*, 2012). Proteins required for stationary interactions or transmigration of the bacteria to escape

Received 2 December, 2014; revised 13 January, 2015; accepted 15 January, 2015. *For correspondence. E-mail jcoburn@mcw.edu; Tel. (+1) 414 955 4116; Fax (+1) 414 955 6567.
†Present address: Department of Medical Microbiology and Immunology, University of Wisconsin, Madison, WI 53706, USA.

from the vasculature and invade surrounding tissues have yet to be mechanistically identified.

P66 is an outer surface protein of *B. burgdorferi* that was identified *in vitro* as a ligand for β_3 and at least some β_1 integrins (Coburn *et al*., 1993; 1998; Behera *et al*., 2008) and as a porin (Skare *et al*., 1997; Pinne *et al*., 2007; Bárcena-Uribarri *et al*., 2010). P66 is required for infectivity in mice (Ristow *et al*., 2012), but not ticks, consistent with its expression pattern (Cugini *et al*., 2003). Structural predictions as well as detergent phase partitioning and efflux of fluorescent dye from liposomes treated with P66 suggest formation of a transmembrane β-barrel (Kenedy *et al*., 2014), although the crystal structure has not yet been solved. The *Δp66* bacteria inoculated by subcutaneous or intradermal injection are cleared from the site of inoculation within 48 h post-inoculation and cannot be recovered from any disseminated sites of infection even within short time periods after infection (Ristow *et al*., 2012). This rapid clearance suggests involvement of the innate immune system, but the infectivity of *Δp66* bacteria was not rescued in mice deficient in either TLR2 or MyD88, signalling molecules known to participate in control of *B. burgdorferi* infection (Ristow *et al*., 2012). The numbers of monocytes, neutrophils and other cells of the host defence system at the inoculation site did not differ in mice inoculated with *Δp66* bacteria as opposed to the wild-type (WT) parental strain (Ristow *et al*., 2012), suggesting that the clearance of the *Δp66* bacteria is mediated through host defences already in place, as opposed to defence cells that migrate to the site of infection. Microarray studies comparing endothelial cell responses to *B. burgdorferi* revealed an up-regulation of the vascular endothelial growth factor/vascular permeability factor pathway in cells incubated with WT bacteria compared with those incubated with *Δp66* bacteria (LaFrance *et al*., 2011). This result suggested that one function of P66 might be to facilitate bacterial transmigration across endothelial barriers.

Previous work identified a portion of P66 [amino acids (a.a.) 142–384] that contains all the sequences required for integrin-binding activity, and a synthetic peptide corresponding to a.a. 203–209 within that region significantly competed with intact *B. burgdorferi* for binding to $\alpha_{IIb}\beta_3$ (Defoe and Coburn, 2001). No other peptides covering the region of a.a. 142–384 significantly or reproducibly inhibited integrin binding. A synthetic peptide representing a.a. 203–209 in content, but in scrambled order, also did not affect integrin binding of *B. burgdorferi*. Although P66 does not contain the traditional consensus arginine-glycine-aspartic acid (RGD) tripeptide sequence of mammalian integrin ligands, in which the aspartic acid residue is critical, a.a. 205 and 207 are both aspartic acids. Synthetic peptides generated with mutations of either a.a. 205 or 207 to alanine were unable to compete with intact *B. burgdorferi* for binding to $\alpha_{IIb}\beta_3$ (Defoe and Coburn, 2001). Maltose-binding protein (MBP)-P66 fusion proteins were constructed with mutations at a.a. 205 or 207 (LaFrance *et al*., 2011). A severe defect of MBP-P66 fusion binding to purified $\alpha_{IIb}\beta_3$ was observed when a.a. 207 was mutated to alanine, and to a lesser extent, binding was reduced when a.a. 205 was mutated to alanine (LaFrance *et al*., 2011). As the tools to perform genetic mutations in *B. burgdorferi* advanced, disruption of *p66* expression in a high-passage, non-infectious strain background of *B. burgdorferi* was performed by replacement of a portion of *p66*, including the putative integrin-binding region, with a kanamycin resistance cassette (Coburn and Cugini, 2003). These mutants were defective in binding to a cell line stably transfected to express $\alpha_v\beta_3$ as compared with WT bacteria.

The goal of this work was to determine if the integrin-binding function of P66 contributes to *B. burgdorferi* infection *in vivo*. We examined the role of P66 in transendothelial migration *in vitro* and in dissemination *in vivo*, and found that integrin binding by P66 is important to both activities of *B. burgdorferi*. The role of P66 in efficient dissemination is biologically significant in light of the natural transmission cycle required to maintain the bacteria in wildlife reservoirs, and is relevant to the development of disseminated disease in accidental hosts such as humans.

Results

Infectivity of WT or Δp66 *bacteria is not altered in* β_3 *chain integrin-deficient mice*

P66 has been shown to bind both β_1 and β_3 chain integrins *in vitro* (Coburn *et al*., 1993; 1998; Coburn and Cugini, 2003; Behera *et al*., 2008). To assess the importance of the interaction of P66 with β_3 chain integrins *in vivo*, mice deficient in β_3 chain integrin expression ($\beta_3^{-/-}$) were utilized. Unfortunately, β_1 integrin chain deficiency results in early embryonic lethality (Stephens *et al*., 1995), precluding testing of mice deficient in this subfamily of integrins. Although $\beta_3^{-/-}$ mice are viable, they have increased vascular permeability and prolonged bleeding times compared with WT mice due to defects in platelet aggregation (Hodivala-Dilke *et al*., 1999). We hypothesized that if the interaction of P66 with β_3 chain integrins was critical for *B. burgdorferi* infection and dissemination, WT *B. burgdorferi* would be non-infectious in $\beta_3^{-/-}$ mice. Alternatively, if the interaction of P66 with β_3 chain integrins serves to down-regulate a negative host response to the bacteria, in the absence of β_3 chain integrins, the presence of P66 should not be required. To test these hypotheses, the ID_{50} of B31-A3 (WT) or *Δp66* bacteria was determined in $\beta_3^{+/+}$ or $\beta_3^{-/-}$ mice after subcutaneous

inoculation at a range of doses. At 4 weeks post-inoculation, the site of inoculation, heart, tibiotarsal joint and ear were collected for analysis by culture and qPCR. ID_{50} determinations were based on *B. burgdorferi* outgrowth in the cultures and were calculated as previously described (Supporting Information Table S1) (Reed and Muench, 1938). Wild-type bacterial loads were similar in both $\beta_3^{+/+}$ and $\beta_3^{-/-}$ mice, whereas *Δp66* bacteria were undetectable in either mouse strain (Supporting Information Fig. S1). These results demonstrate that *B. burgdorferi* interaction with β_3 chain integrins, specifically, is not critical to infection in mice.

Amino acids 202–208 of P66 are important for binding to β_3 chain integrins but are not critical to porin function

Although the interaction of P66 with β_3 chain integrins is not required for infection of mice, the function of P66 as an integrin ligand may still be critical to its role in the ability of *B. burgdorferi* to establish infection, given that the recombinant protein and the bacteria do bind to additional integrins. To further investigate the roles of the P66 sequences previously implicated in adhesion *in vitro*, recombinant MBP-P66 fusion proteins were constructed with mutations in the putative integrin-binding region at aspartic acid residues 205 and 207 to alanine (D205A,D207A), or a deletion of seven amino acids (Del202–208), spanning the critical portion of the putative integrin-binding region (Fig. 1A).

In parallel, the same mutations were introduced into non-infectious (high-passage HB19 clone 1) and infectious (B31-A3) *B. burgdorferi* strain backgrounds. *Borrelia burgdorferi* HB19 clone 1 (HB19-1) is a high-passage, non-infectious derivative of a clinical isolate of *B. burgdorferi* with significant loss of genomic elements compared with infectious strain backgrounds. This results in the expression of many fewer adhesins and lower background ELISA signals in adhesion assays compared with infectious strain backgrounds and is a useful tool for *in vitro* studies. Previous work had demonstrated that HB19-1 *Δp66* binds less efficiently than the parental strain to HEK293 cells stably expressing human integrin $\alpha_v\beta_3$ (293 + $\alpha_v\beta_3$) (Coburn and Cugini, 2003). Surface expression of the mutant forms of P66 in both the non-infectious (HB19-1, Fig. 1B) and infectious (B31-A3, Fig. 1C) strain backgrounds was confirmed by Western blot after proteinase K treatment of the bacteria. Notably, both mutant forms were very similar to the WT form of P66 in terms of the fragments generated as determined by the banding pattern of the digested protein, with a doublet formed at approximately 54 and 55 kDa for the mutant as well as WT forms of the protein. The Del202–208 protein did however appear somewhat more sensitive to proteolysis, as the P66 bands were undetectable at the highest

A

Mutations within P66 integrin-binding region

	200	201	202	203	204	205	206	207	208	209	210
P66-WT	AGA	AAT	CAA	GAG	AAT	GAC	AAA	GAC	ACT	CCA	TAC
	R	N	Q	E	N	D	K	D	T	P	Y
D205A, D207A	AGA	AAT	CAA	GAG	AAT	G***C***C	AAA	G***C***C	ACT	CCA	TAC
	R	N	Q	E	N	***A***	K	***A***	T	P	Y
Del202-208	AGA	AAT	---	---	---	---	---	---	---	CCA	TAC
	R	N	-	-	-	-	-	-	-	P	Y

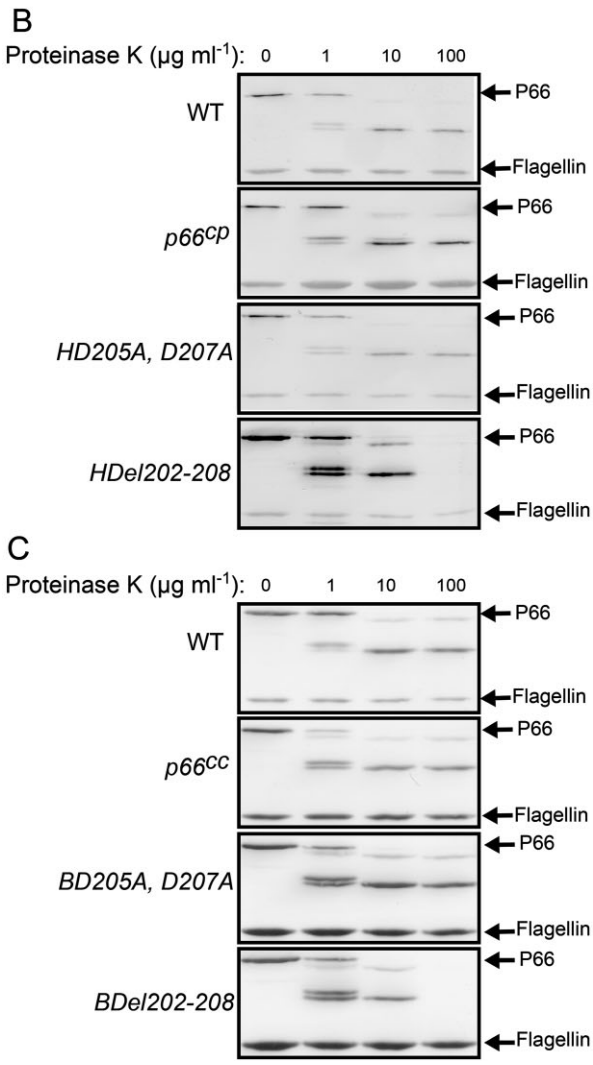

Fig. 1. Genotype and phenotype of P66 integrin-binding region mutants.
A. Nucleotide and amino acid sequence of WT, D205A,D207A and Del202–208 strains. Mutations in the nucleotide sequence that resulted in altered amino acids are in bold and italics for mutations at a.a. 205 and 207. Nucleotides removed from the coding region are represented as dashes for Del202–208.
B and C. Surface expression of P66 in various *Borrelia burgdorferi* strains (B: HB19 strains, C: B31-A3 strains). The bacterial strains were incubated with varying concentrations of proteinase K (1, 10, 100 μg ml^{-1}) for 1 h. Untreated bacteria were used as a negative control. Bacterial lysates were run on a 10% SDS-PAGE gel and transferred to an Immobilon membrane that was probed with antibodies to P66 and flagellin. Colorimetric methods were used for visualization. cp = *p66* gene restored on a shuttle plasmid, cc = *p66* gene restored to endogenous locus on chromosome.

proteinase K concentration. Nevertheless, the proteinase K digestion of all P66 variants demonstrated that the protein was exposed on the surface of the bacteria. Flagellin was used as a control for intact bacteria, as the protein is periplasmic in *B. burgdorferi*, and therefore is not accessible to the protease in intact bacteria.

Although the mutations resulting in a substitution of aspartic acid to alanine at a.a. 205 and 207 are predicted to be relatively minor in terms of effects on overall protein structure, the deletion of seven amino acids to create the Del202–208 mutants has the potential to cause a significant change in the protein structure. To determine whether these mutations affected the other known function of P66, i.e. channel formation, a planar lipid bilayer assay was used to assess the ability of P66 purified from strains expressing targeted P66 mutants to assemble and form a functional porin. Previous work described the loss of the P66 channel-forming activity (~11 ns in 1 M KCl) in *B. burgdorferi* when outer membrane porins were purified from *Δp66* bacteria compared with WT bacteria (Pinne *et al*., 2007). For this work, the native proteins were purified from the overexpressing, non-infectious HB19 strain background for assessment. No differences were observed in the channel size between P66 with targeted mutations and WT P66 (Fig. 2), although fewer pores were formed by the D205A,D207A mutant. In addition, the activity of a different channel at ~5 ns may have been affected in the D205A,D207A mutant. The reason for this is unclear, given that the deletion of a.a. 202–208 did not affect either the number of channels formed or the activity of the other former channel. However, both site-directed mutant versions of P66 formed the 11 ns channels in the planar lipid bilayer system, demonstrating that the structures of the proteins were not grossly disrupted in the context of the *B. burgdorferi* outer membrane. These data are supported by the appearance of a band of ~480 kDa that co-migrated with the WT protein when the site-directed mutant proteins were analysed by blue native gel electrophoresis (data not shown). Structural predictions using PRED-TMBB (Bagos *et al*., 2004) did not suggest gross alterations of the protein due to the site-directed changes, although definitive analyses of possible effects on the overall structure of the mutated versions of P66 await crystal structure determination.

The abilities of WT and mutant recombinant forms of the integrin-binding domain of P66 (P66M) to bind $\alpha_v\beta_3$ were assessed *in vitro* using both purified $\alpha_v\beta_3$ and cells overproducing this integrin. The binding affinity (K_D) of human integrin to WT MBP-P66 was ~1370-fold greater than that of the Del202–208 protein and ~225-fold greater than that of the D205A,D207A protein as assessed by surface plasmon resonance (SPR) (Table 1). Similarly, the binding of mouse integrin to WT P66 indicated by K_D values was ~1320-fold more efficient than that of the

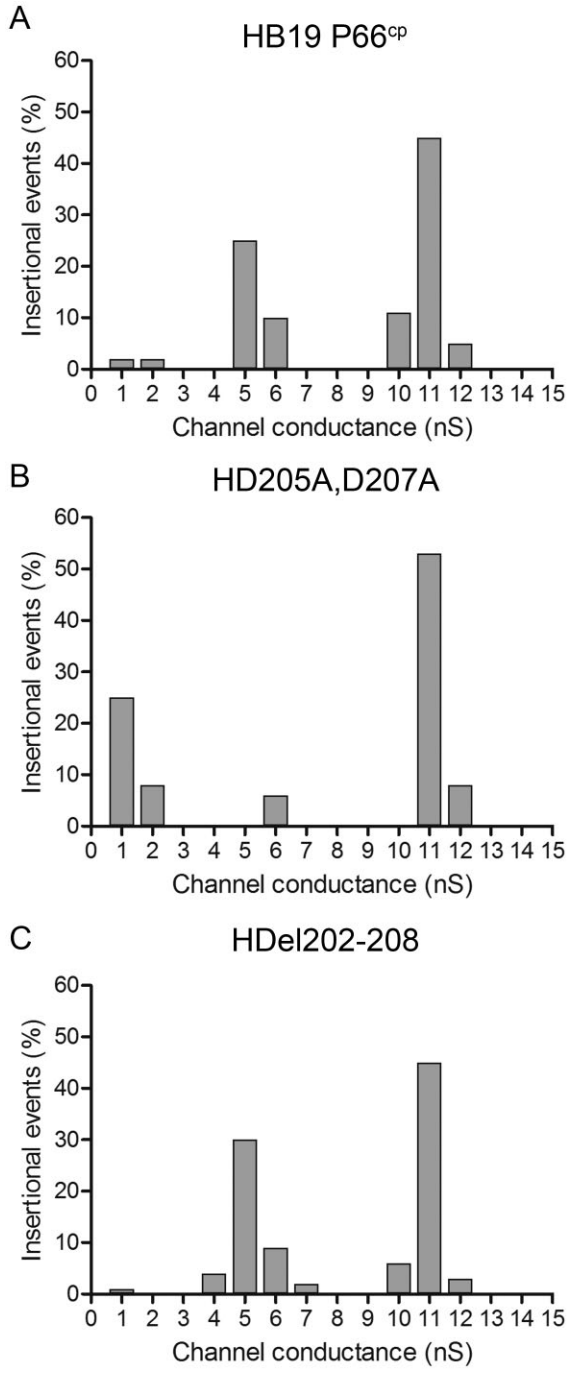

Fig. 2. Targeted mutation of the integrin-binding region of P66 does not affect pore formation. Histograms show pore-forming activities of P66 isolated from *Borrelia burgdorferi* HB19 *p66cp* (A), *HD205A,D207A* (B), or *HDel202–208* (C) in a diphytanoyl phosphatidylcholine/n-decane (PC) membrane. The bathing solution was 1 M KCl. The total number of insertional events was 100 for HB19 *p66cp*, 100 for *HDel202–208* and 36 for *HD205A,D207A*. The experiment was performed in triplicate for all strains, with one representative shown. The typical single channel conductance activity for P66 (11 nS) was observed in outer membrane protein preparations from all three *B. burgdorferi* strains.

Table 1. MBP-P66 site-directed mutant proteins differ in binding to integrin $\alpha_v\beta_3$.

MBP-P66 variant	Ligand	K_D (μM)	k_{on} (10^3 s^{-1} M^{-1})	k_{off} (10^{-1} s^{-1})
P66M	Human $\alpha_v\beta_3$	0.13 ± 0.06[a]	321.33 ± 115.18	0.31 ± 0.05
	Mouse $\alpha_v\beta_3$	0.20 ± 0.04[a]	111.56 ± 32.49	0.20 ± 0.01
D205A,D207A	Human $\alpha_v\beta_3$	29.28 ± 6.76[a,b]	0.71 ± 0.18[a]	0.19 ± 0.10[a]
	Mouse $\alpha_v\beta_3$	20.34 ± 5.90[a,b]	1.45 ± 0.39[a]	0.25 ± 0.04[a]
Del202–208	Human $\alpha_v\beta_3$	178.33 ± 27.35[a,b]	0.09 ± 0.01[a]	0.17 ± 0.01[a]
	Mouse $\alpha_v\beta_3$	264.29 ± 147.34[a,b]	0.13 ± 0.06[a]	0.18 ± 0.01[a]
MBP-βgal	Human $\alpha_v\beta_3$	n.b.[c]	n.b.[c]	n.b.[c]
	Mouse $\alpha_v\beta_3$	n.b.[c]	n.b.[c]	n.b.[c]

a. The K_D values were obtained from the average of every k_{off} divided by every k_{on} from each run.
b. Because the binding of D205A,D207A or Del202–208 to mouse or human integrin $\alpha_v\beta_3$ is weak, the determined values should be considered estimates.
c. No binding activity was detected.
All values represent the mean ± SEM of three experiments.

Del202–208 mutant and ~100-fold more efficient than that of the D205A,D207A protein (Table 1). However, there were no significant differences between mouse and human integrins in binding to the same recombinant P66 proteins ($P = 0.92$) (Table 1). Similar trends for the changes in K_Ds were also seen using an ELISA-based approach (data not shown). These results suggest that the D205A,D207A and the Del202–208 mutant proteins each had reduced binding to purified integrin $\alpha_v\beta_3$, and that the reduction in integrin binding to the D205A,D207A mutant protein was less severe than to the Del202–208 mutant protein.

To assess binding of the mutant forms of P66 to integrin $\alpha_v\beta_3$ in the context of intact host cells, confluent monolayers of 293 + $\alpha_V\beta_3$ cells were probed with the recombinant forms of P66. After unbound proteins were removed by washing, bound proteins were fixed and quantified by ELISA. ELISA signal was normalized to cell retention assessed by crystal violet staining, and signals were normalized to P66M (WT). MBP-fusion proteins D205A,D207A and Del202–208 bound significantly less to 293 + $\alpha_V\beta_3$ cells when compared with WT P66M binding to 293 + $\alpha_V\beta_3$ cells (Fig. 3A).

The deficiency in integrin binding observed with targeted mutants of P66 in recombinant form was also investigated in the context of intact bacteria. HB19-1*Δp66* bacteria were previously shown to be deficient in binding to integrin $\alpha_V\beta_3$ (Coburn and Cugini, 2003). In the current study, both the HB19-1 (WT) and complemented derivatives expressing WT P66 (WT and *p66*^{cp}) bound to 293 + $\alpha_V\beta_3$ cells at similar levels. In contrast, *HD205A,D207A* and *HDel202–208* bacteria both bound significantly less to 293 + $\alpha_V\beta_3$ cells than did WT bacteria or *p66*^{cp} bacteria (Fig. 3B), and bound to the cells at efficiencies similar to that of the HB19-1*Δp66* bacteria relative to the parental strain (Coburn and Cugini, 2003). Together with the channel-forming results presented above, these results demonstrated that the two *in vitro* identified functions of P66 (integrin binding and 11 ns pore formation) can be separated to allow specific assessment of the integrin-binding function without grossly affecting porin activity.

The integrin-binding region of P66 is not critical for establishment of B. burgdorferi *infection after subcutaneous inoculation*

The infectivity phenotype of the site-directed mutant forms of P66 was examined by ID_{50} determinations. C3H/HeN mice were inoculated with B31-A3 (WT), *Δp66*, *BD205A,D207A* or *BDel202–208* bacteria at a range of doses. At 4 weeks post-inoculation, tissues, including the heart, tibiotarsus, inoculation site skin and ear, were harvested for culture and qPCR determination of bacterial load. ID_{50} determinations were based on infection status of cultures and were calculated as previously described (Reed and Muench, 1938). All strains bearing mutations in *p66* had ID_{50} values comparable to WT bacteria with the exception of one clone of *BDel202–208* (Table 2). That clone may have had additional mutations in the genome beyond the mutant P66, but we did verify that all genomic plasmids present in the parental strain were present in the mutant as detected by end point PCR on the day of inoculation into mice. Despite the aberrant ID_{50} of one mutant clone, these results clearly demonstrate that WT levels of β_3 chain integrin binding are not required for *B. burgdorferi* to establish disseminated infection at 4 weeks post-inoculation. More importantly, these results demonstrate that the complete loss of infectivity of the *Δp66* mutant clones (Ristow *et al.*, 2012) is due to at least one additional function of P66 (e.g. pore formation, specifically when the bacteria are not in a protected environment) that is important for *B. burgdorferi* infection.

In agreement with the ID_{50} values, inoculation with *BD205A,D207A* clones resulted in similar bacterial burdens in most tissues assessed compared with WT inoculated mice (Fig. 4). Bacterial burdens in the hearts of

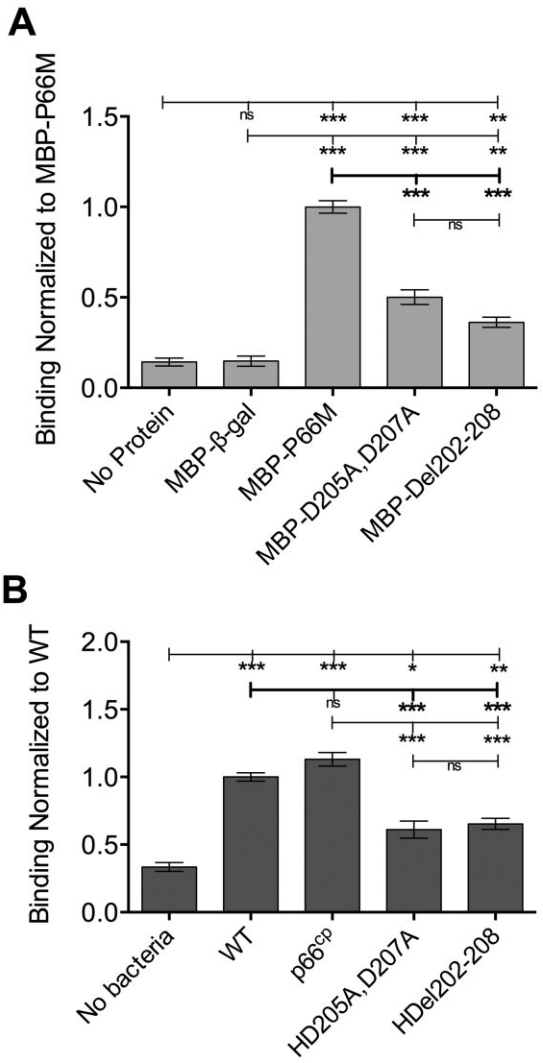

Fig. 3. Targeted mutation of the integrin-binding region of P66 significantly reduces binding to cells expressing $\alpha_v\beta_3$ integrin.
A. Up to 0.1 μM recombinant protein was incubated with 293 + $\alpha_v\beta_3$ cells grown to confluence in 96-well plates for 1 h before washing and fixation of bound protein. Bound protein was quantified by ELISA using anti-MBP as primary antibody, and anti-rabbit-HRP conjugate as secondary. Developed plates were read at 655 nm. ELISA signal was normalized to crystal violet staining of the wells and results were normalized to MBP-P66M.
B. 1.25×10^6 HB19-1 (wild-type) and derivative bacteria per well were incubated with cells for 1 h before completing the assay as above, substituting anti-Lyme spirochete as primary antibody. Results were normalized to wild type. Mean and standard error of measurement are indicated. Statistical analyses were performed using one-way ANOVA Kruskal–Wallis test with Dunn's multiple comparison post-test. $^*P < 0.05$, $^{**}P < 0.01$, $^{***}P < 0.001$.

mice inoculated with *BD205A,D207A* or *BDel202–208* were significantly lower than those of WT inoculated mice. In addition, mice inoculated with *BDel202–208* bacteria had significantly lower bacterial burdens in the tibiotarsal joint compared with WT or *BD205A,D207A* inoculated mice. At the site of inoculation, *BD205A,D207A* bacteria were observed at levels similar to WT bacteria, but were significantly higher than those of *BDel202–208* inoculated mice. The differences in bacterial burdens between the strains producing the two different mutated versions of P66 indicate that there is a more substantial colonization defect in the *BDel202–208* mutant. This result suggests that although pore formation is not affected, the difference in affinities of the mutant proteins for purified mouse $\alpha_v\beta_3$ observed *in vitro* correlates with the ability of *B. burgdorferi* to colonize tissues in mice.

The integrin-binding region of P66 promotes endothelial transmigration of B. burgdorferi *in vitro*

The effect of the Del202–208 mutation on *B. burgdorferi* burdens in some tissues suggests a potential defect in at least some steps in the complex dissemination process. The spread of *B. burgdorferi* to tissues distant from the site of inoculation may occur by migration through tissues without entry into the vasculature, but is likely to be facilitated by entry into and dissemination through the vasculature. Colonization of distal sites would then involve crossing endothelial barriers while the bacteria are entering and exiting the vascular system. The potential role of the integrin-binding function of P66 in the ability to cross endothelial cell monolayers was therefore investigated *in vitro* based on the Boyden chamber assay (Boyden, 1962). A microvascular endothelial cell line (HMEC-1) was used to represent the cells present in small vessels or capillary beds *in vivo*, where *B. burgdorferi* can successfully exit the vasculature (Moriarty *et al.*, 2008; 2012). Bacterial transmigration was assessed using confluent layers of HMEC-1 cells in Transwell inserts. Transwells without cells were used as controls for bacteria crossing the membrane alone. The role of P66 in this activity was quantified by comparing the ability of B31-A3 (WT), *Δp66*, *p66^{cc}*, *BD205A,D207A* and *BDel202–208* bacteria to cross the cell monolayer at a multiplicity of infection (MOI) of 20. Migration of all *B. burgdorferi* strains

Table 2. Subcutaneous ID_{50} determinations of *p66* site-directed mutants 4 weeks post-inoculation.

Bacterial strain	Doses (number of motile bacteria per mouse[a])	ID_{50} value
B31-A3 (wild type)	10^1–10^9	4.64×10^2–2.37×10^4
Δp66 C3–14	10^1–10^9	$>10^9$
BD205A,D207A clone 2–9	10^1–10^9	1.78×10^4
BD205A,D207A clone 2–30	10^1–10^9	5.62×10^3
BD205A,D207A clone 3–32	10^1–10^9	5.62×10^3
BDel202–208 clone 3	10^1–10^9	1×10^4
BDel202–208 clone 29	10^1–10^9	1×10^4
BDel202–208 clone 78	10^1–10^9	4.64×10^6

a. Five mice were inoculated per dose per bacterial strain.

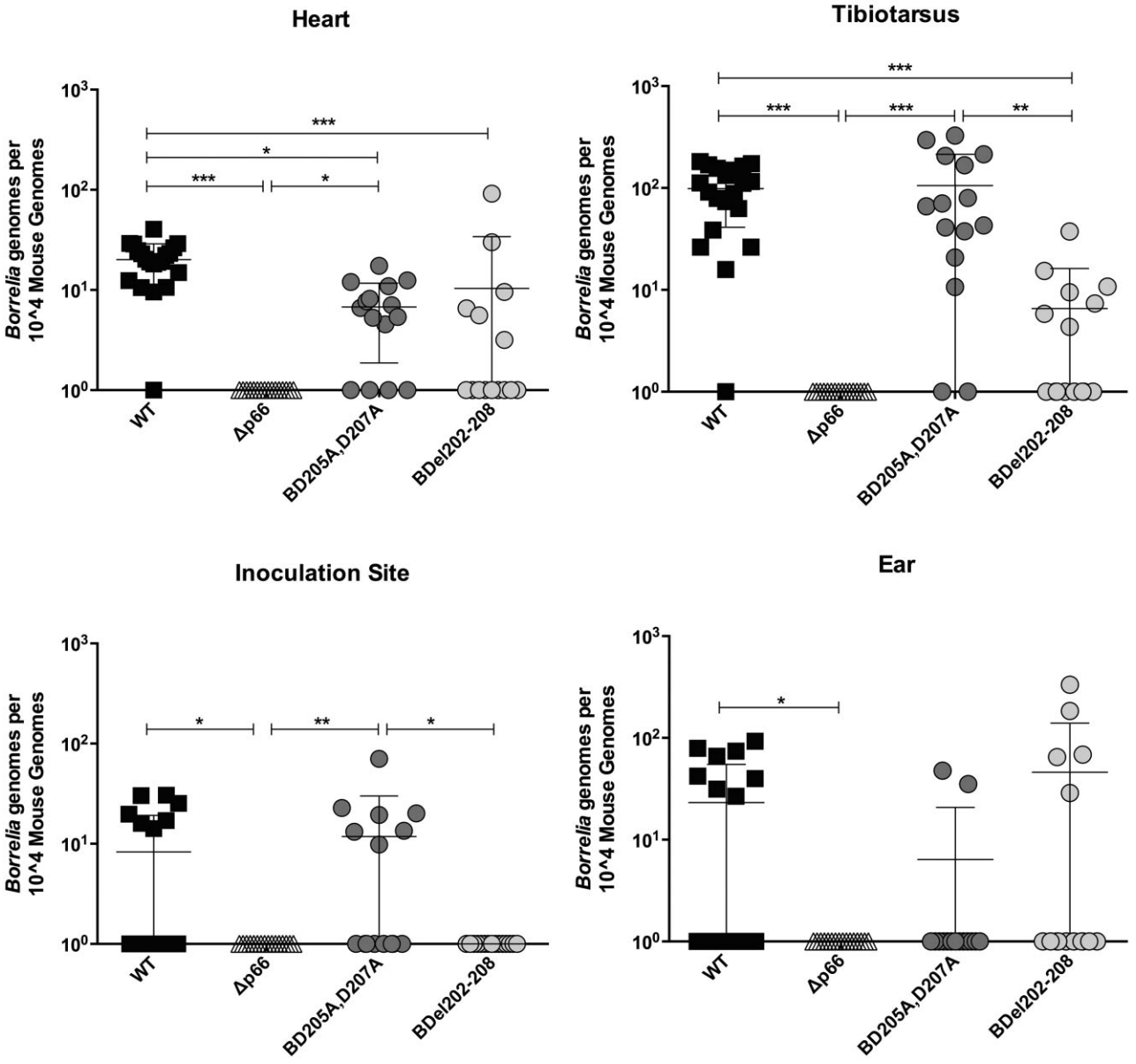

Fig. 4. Targeted mutation of P66 alters dissemination of *Borrelia burgdorferi* following subcutaneous inoculation. C3H/HeN mice were inoculated with a range of doses (10^1–10^9 per mouse) of B31-A3 (wild-type), *Δp66*, *BD205A,D207A* or *BDel202–208* bacteria. Tissues were harvested 4 weeks post-inoculation and total DNA was purified and analysed by qPCR with primers to detect *Borrelia* genomes or mouse genomes. Bacterial burdens from mice inoculated with 10^5 bacteria are shown. Mean bacterial load is indicated with error bars representing standard deviation. Statistical analyses were performed using a one-way ANOVA Kruskal–Wallis test with Dunn's multiple comparison post-test. $^*P < 0.05$, $^{**}P < 0.01$, $^{***}P < 0.001$. $n \geq 5$ mice per strain.

in wells without cells was significantly higher than that of any strain crossing wells with a HMEC-1 cell monolayer at time points ≥24 h (data not shown). By 48 h, there was a significant defect in the ability of *Δp66* bacteria to cross the cell monolayer compared with WT and *p66*^{cc} bacteria (Fig. 5). A similar defect was observed in *BDel202–208* bacterial transmigration of the cell monolayer compared with WT and *p66*^{cc} bacteria. The ability of the *BD205A,D207A* bacteria to cross the cell layers was not significantly different from that of WT bacteria, consistent with the decreased severity of phenotypic effects *in vivo* in this mutant as compared with the *BDel202–208* bacteria and with the *in vitro* integrin-binding results. Transmigration was analysed up to 72 h post-inoculation, but the health of all *B. burgdorferi* strains diminished after 48 h in the cell growth medium, which is relatively nutrient poor compared with the bacterial culture medium, and results were not reproducible after 48 h.

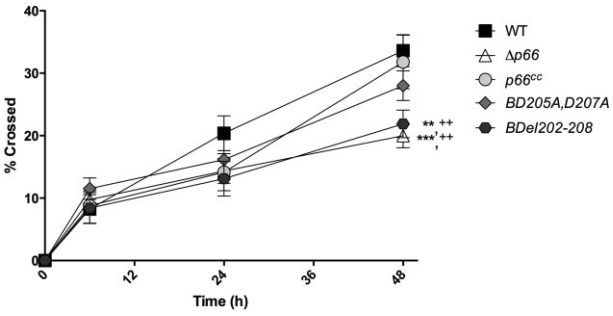

Fig. 5. Mutation of P66 affects the ability of *Borrelia burgdorferi* to cross an endothelial monolayer of cells. HMEC-1 human microvascular endothelial cells were plated in 3 μm pore size Transwell inserts and grown to confluence in antibiotic free medium. B31-A3 (wild-type), *Δp66*, *p66*^{cc}, *BD205A,D207A* or *BDel202–208* bacteria were added to the insert at an MOI of 20 and the ability of bacteria to cross the monolayer of cells was assessed over 48 h by taking an aliquot from the insert and from the well below. Bacteria were counted manually using a Petroff-Hausser counting chamber under dark-field microscopy, and the percentage of bacteria that crossed the cell monolayer was calculated. Inserts without a cell monolayer were assessed as controls for bacterial crossing of the membrane alone. A two-way repeated measures ANOVA with Bonferroni's post-test was performed. Asterisks indicate comparison to wild-type bacteria, plus signs indicate comparison to *p66*^{cc} bacteria. $^{**/++}P < 0.01$, $^{***}P < 0.001$, $n = 5$.

Decreased integrin-binding activity of P66 delays B. burgdorferi *dissemination from the vasculature*

In the context of infectivity and dissemination, the ability of integrin-binding deficient mutants to cross endothelial layers *in vivo* and exit the vasculature was quantified in multiple tissues by performing an ID_{50} determination after intravenous inoculation. C3H/HeN mice were retro-orbitally inoculated with a range of doses of B31-A3 (WT), *Δp66*, *p66*^{cc} or *BDel202–208* bacteria. After 2 weeks, tissues were harvested for culture and qPCR, including the heart, tibiotarsal joint, skin between the scapulae and ear. ID_{50} determinations were based on bacterial outgrowth in cultures and were calculated as previously described (Table 3). The ID_{50} of WT bacteria was slightly higher when the bacteria were inoculated *via* the intravenous route as compared with subcutaneous inoculation (compare Tables 2 and 3). Within the intravenous inoculation model, *p66*^{cc} bacteria had a similar ID_{50} to WT bacteria, but the *Δp66* and *BDel202–208* bacteria were not recovered at 2 weeks post-inoculation (Table 3). Bacterial loads assessed by qPCR confirmed culture results in that mice inoculated with WT or *p66*^{cc} bacteria had similar bacterial loads in all tissues observed, while *Δp66* and *BDel202–208* bacteria were not detected by either culture or qPCR at 2 weeks post-inoculation (Table 3 and Fig. 6A). Interestingly, when infections were allowed to progress for 4 weeks post-intravenous inoculation, the *BDel202–208* bacteria and *BD205A,D207A* bacteria were as infectious as WT bacteria by ID_{50} determination (Table 3). Although infectivity was similar between all strains at 4 weeks post-inoculation, bacterial burdens were variable in some tissues, as determined by qPCR (Fig. 6B). Unlike the defect in tissue colonization observed in the tibiotarsus and ear after subcutaneous inoculation, *BDel202–208* bacteria were observed at WT levels in all tissues except the heart, where the bacterial load was significantly lower than that of WT bacteria following intravenous inoculation. In the tibiotarsal joint, the *BD205A,D207A* bacterial burden was significantly higher than *Δp66* and *BDel202–208* bacterial burdens, but not significantly different from WT bacterial burdens. In the skin between the scapulae, the *p66*^{cc} bacterial burden was significantly higher than *Δp66* and *BD205A,D207A* bacterial burdens, but not significantly different from WT bacterial burdens. The observed delay in colonization of tissues by the *BDel202–208* bacteria following intravenous inoculation may explain the variation in bacterial burdens, as *BDel202–208* and potentially *BD205A,D207A* bacteria may have yet to establish a stable bacterial burden for maintenance of the bacteria. The more severe colonization defect of the *BDel202–208* mutant as compared with the *BD205A,D207A* strain also correlates with the more severe loss of affinity of the recombinant proteins in integrin binding as determined by SPR.

Discussion

In this work, we tested the hypothesis that the infectivity defect of the *Δp66* mutants is due to an inability to disseminate from the site of infection into other tissues, where the bacteria reside in extravascular connective

Table 3. Intravenous ID_{50} determinations of *p66* site-directed mutants.

Bacterial strain	Doses (number of motile bacteria per mouse[a])	Weeks post-inoculation	ID_{50} value
B31-A3 (wild type)	10^3–10^7	2	4.64×10^4
		4	2.31×10^4
Δp66 C3–14	10^3–10^7	2	$>10^7$
		4	$>10^7$
C3–14^{cc} clone 23	10^3–10^7	2	2.15×10^5
		4	5.62×10^5
BD205A,D207A clone 2–30	10^3–10^7	4	2.15×10^5
BD205A,D207A clone 3–32	10^3–10^7	4	4.64×10^4
BDel202–208 clone 3	10^3–10^7	4	5.62×10^5
BDel202–208 clone 29	10^3–10^7	2	$>10^7$
		4	1×10^6

a. Five mice were inoculated per dose per bacterial strain.

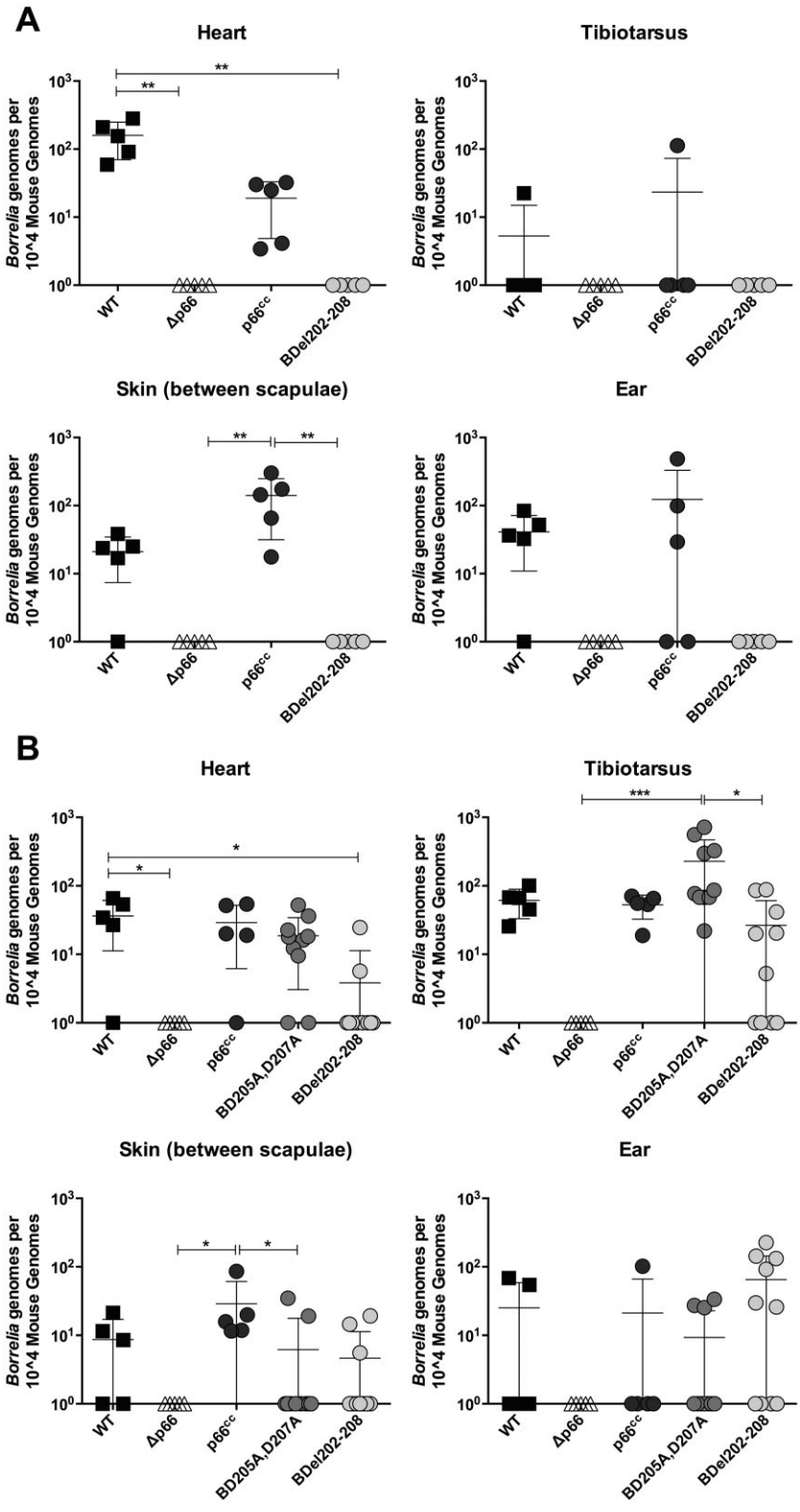

Fig. 6. Targeted mutation of residues involved in integrin binding by P66 delays dissemination of *Borrelia burgdorferi* following intravenous inoculation. C3H/HeN mice were inoculated retro-orbitally with a range of doses (10^3–10^7 per mouse) of B31-A3 (wild-type), *Δp66*, *p66^{cc}*, *BD205A,D207A* or *BDel202–208* bacteria. Tissues were harvested 2 weeks (A) or 4 weeks (B) post-inoculation and total DNA was purified and analysed by qPCR with primers to detect *Borrelia* genomes or mouse genomes. Bacterial burdens from mice inoculated with 10^7 bacteria are shown. Mean bacterial load is indicated with error bars representing standard deviation. Statistical analyses were performed using a one-way ANOVA Kruskal–Wallis test with Dunn's multiple comparison post-test. $^*P < 0.05$, $^{**}P < 0.01$, $^{***}P < 0.001$. $n = 5$ mice per group.

tissue. The inability to escape the site of inoculation or from the bloodstream might effectively render the bacteria more susceptible to antimicrobial factors in the mouse skin or bloodstream. Although it is difficult to visualize bacterial entry into the circulation, we did demonstrate a defect in transendothelial migration by the *Δp66* strains *in vitro* (three independent clones), and that *B. burgdorferi* strains producing a mutant P66 with drastically reduced affinity for integrin $\alpha_v\beta_3$ were phenotypically similar to the *Δp66* strains. A new model, which allows *in vivo* assessment of transmigration of *B. burgdorferi* from the vasculature into the knee joint of mice, is described elsewhere (Kumar *et al.*, submitted). Interestingly, when transmigration of *Δp66* bacteria is compared with WT bacteria following intravenous inoculation, *Δp66* bacteria were deficient in extravasation into the knee joint when assessed at 24 h post-inoculation (Kumar *et al.*, submitted). Consistent with our results, a defect in transendothelial migration into the knee joint of mice was also observed with integrin-binding deficient strains *BDel202–208* and *BD205A,D207A* strains using this *in vivo* method (Kumar *et al.*, submitted). Furthermore, our work revealed that the observed defect in transendothelial migration of integrin-binding deficient *B. burgdorferi* strains translates to a dissemination defect, as demonstrated in this work using both subcutaneous and intravenous inoculation to infect mice. Although the intravenous inoculation model does not recapitulate the natural route of transmission *via* tick bite, it does allow the delivery of known numbers of bacteria, and allows quantification of efficiency of crossing microvascular walls to colonize tissues distant from the inoculation site. Given the differences in the phenotypes of the *D205A,D207A* versus the *Del202–208* strains, at least some of this function may be affected by the a.a. 202–208, or by the different affinities of the mutant versions of P66 for $\alpha_v\beta_3$ or other integrins. Because the *Δp66* bacteria were previously shown to behave much like the WT parental strain when placed inside a dialysis membrane chamber in the peritoneum of rats (Ristow *et al.*, 2012), we thought it unlikely that porin activity is essential to the function of P66 in this protected environment. In addition, no differences in *in vitro* growth have been detected for any of the *p66* mutants in comparison to the WT parental strain. We did test the potential role of P66 in resistance of *B. burgdorferi* to serum (complement), and to phagocytosis by resident macrophages and dendritic cells in the skin (see Supporting Information Appendix S2), but the absence of P66 had no effect in any of these experiments. Together, our data suggest that either the porin activity or an as yet unknown function of P66 contributes to survival of *B. burgdorferi* in mouse infection when the bacteria are not sheltered.

In vivo *function of P66 as an integrin ligand*

To date, P66 is unique among bacterially encoded integrin ligands in that it interacts with the β_3 chain and at least some β_1 chain integrins. Of note, *B. burgdorferi* is an extracellular pathogen that has not been documented to occupy intracellular niches *in vivo*. P66 has been shown to interact with four integrins: $\alpha_{IIb}\beta_3$, $\alpha_v\beta_3$, $\alpha_3\beta_1$ and $\alpha_5\beta_1$ (Coburn *et al.*, 1993; 1998; Behera *et al.*, 2008). The mammalian ligands for these integrins contain an RGD (Arg-Gly-Asp) sequence (reviewed in Barczyk *et al.*, 2010). Invasin, a *Yersinia* species β_1 chain integrin ligand, does not contain an RGD sequence, but binds β_1 chain integrins with 100-fold higher affinity than the native ligand, fibronectin (Tran van Nhieu and Isberg, 1991). It has been demonstrated that invasin contains a critical aspartic acid residue required for entry into host cells (Leong *et al.*, 1995). P66 does not encode an RGD sequence, but within the putative integrin-binding region, the aspartic acid residues at a.a. 205 and 207 may contribute to the specific interaction with integrins. P66 binds to $\alpha_v\beta_3$ with an affinity on the order of that of a vitronectin-derived 15-amino-acid peptide containing the RGD sequence (the K_D for vitronectin was not measurable due to multiple interactions) (Orlando and Cheresh, 1991), and as shown in Table 1, the site-directed mutant P66 proteins bind with considerably lower affinity.

As studies continue to carefully dissect the interactions of *B. burgdorferi* with the mammalian host, the parallels between *B. burgdorferi* exit from the vasculature and those observed in leukocyte interactions and exit from the vasculature are striking. During recruitment to sites of inflammation, neutrophils, monocytes and T-cells engage integrins at various steps in vascular interactions that ultimately lead to transmigration out of the vasculature (reviewed in Herter and Zarbock, 2013). The initial steps in the extravasation of lymphocytes involve lectin–carbohydrate interactions, followed by interactions mediated by integrins of the β_2 chain family (reviewed in Springer, 1994). Initial interactions of *B. burgdorferi* with the vasculature are mediated by BBK32 binding to fibronectin, then GAGs (Moriarty *et al.*, 2012). *Borrelia burgdorferi* interactions with integrins would then be a subsequent step in transmigration through the vascular endothelium to cause infection in extravascular sites in diverse tissues. In both endothelial transmigration events, carbohydrate-mediated interactions precede integrin-mediated interactions. Both leukocyte and *B. burgdorferi* transmigration across the endothelium likely occur at endothelial cell-cell junctions, as *B. burgdorferi* has been observed in the intercellular junctions between endothelial cells (Szczepanski *et al.*, 1990; Moriarty *et al.*, 2008). The P66-integrin interaction may function to initiate

signalling cascades to facilitate transmigration across the endothelium, including VEGF/VPF, as previously reported (LaFrance *et al*., 2011), which would represent a novel function for bacterial integrin ligands. Alternatively, *B. burgdorferi* may use the integrin interactions with P66 as traction in cooperation with the motility of the bacterium to drive through the endothelial barrier.

Multiple functions of P66

Of the *in vitro* identified functions of P66 to date, this work strongly supports the hypothesis that the function of P66 as an integrin ligand is required for endothelial transmigration as a key step in the dissemination of *B. burgdorferi*. P66 is known to bind both of the β_3 chain integrins and at least two β_1 chain integrins. Based on ligand recognition by integrin family members, it is entirely possible that P66 also binds additional α_v integrins. It is clear that, even in the absence of the integrin subunit β_3, P66 would have multiple other targets for attachment. The discrepancy between WT ID_{50}s of integrin-binding deficient strains after subcutaneous inoculation, albeit with some reductions in tissue burdens, and avirulence of *Δp66* bacteria implies an additional function(s) of P66 in *B. burgdorferi* survival in the mouse model. However, this work does highlight the importance of dissemination through the bloodstream in the ability of *B. burgdorferi* to colonize sites distal from the site of the tick bite. Future work will include determination of whether the *Δp66* bacteria can enter the vasculature, and whether integrin binding is required for *B. burgdorferi* entry into the circulation, but the results presented here suggest the possibility of two mechanisms of dissemination that are functionally distinct. One, promoted by P66-integrin interactions, would be more rapid and involve spread through the vasculature. The other, which does not involve integrin binding by P66, is slower and may rely more on the motility of the bacteria and interactions with the tissue matrix than on P66 integrins as seen in the intravascular stage. Future studies will be informed by the work presented here, in which we have demonstrated for the first time the requirement for integrin-binding function in efficient bacterial dissemination, and in particular a role for P66 in dissemination of *B. burgdorferi in vivo*, a property that would facilitate maintenance of the bacteria in the enzootic cycle and that is significant to the pathogenesis of Lyme disease.

Experimental procedures

Bacterial strains and growth conditions

Bacterial strains and plasmids used in this work are described in Supporting Information Table S2. *Borrelia burgdorferi* B31-A3 strains and derivatives (Elias *et al*., 2002) were grown in BSK II medium (Barbour-Stoenner-Kelly II; Barbour *et al*., 1983). HB19 (human blood isolate 19) strains and derivatives were grown in MKP medium (modified Kelly-Pettenkofer; Preac-Mursic *et al*., 1986), which we had previously found to maximize binding to the platelet integrin $\alpha_{IIb}\beta_3$ (Coburn *et al*., 1994). Media were supplemented with 15 g l^{-1} agar (for *Escherichia coli*) or 6.8 g l^{-1} agarose (for *B. burgdorferi*; Samuels, 1995). The genomic plasmid content of all *B. burgdorferi* cultures to be injected into mice was assessed by PCR (Elias *et al*., 2002; Bunikis *et al*., 2011) to ensure retention of all plasmids in the parental strain immediately prior to the mouse infections. Growth of *B. burgdorferi* from mouse tissues was in BSK II medium supplemented with rifampicin to 50 μg ml^{-1}, amphotericin B to 2.5 μg ml^{-1} and phosphomycin to 20 μg ml^{-1}.

Mice

The Institutional Animal Care and Use Committee of the Medical College of Wisconsin approved all work with animals. The protocol numbers are AUA2263 and AUA0488. C3H/HeN mice were purchased at the age of 3 weeks from Charles River Laboratories. $\beta_3^{-/-}$ mice and $\beta_3^{+/+}$ WT littermates were originally obtained from Dr Richard O. Hynes (Massachusetts Institute of Technology) and maintained at the Medical College of Wisconsin. Mice were fed and watered *ad libitum* throughout the experiments. Mice were euthanized by controlled CO_2 administration followed by cardiac puncture.

Bacteria were prepared for syringe inoculation experiments as described previously (Ristow *et al*., 2012). Briefly, laboratory-cultured *B. burgdorferi* were cultivated to a concentration of $1–5 \times 10^7$ bacteria per ml. For every experiment, plasmid content of each strain was assessed at the morning of infection by PCR as previously described (Bunikis *et al*., 2011), and strains retaining all parental plasmids were subjected to several rounds of centrifugation and washes to concentrate the bacteria and remove the protein-rich medium in which the bacteria are grown. After suspension in phosphate-buffered saline (PBS) + 0.2% normal mouse serum (NMS), the bacteria were counted and diluted to the desired concentrations for inoculation.

For ID_{50} determinations, mice were inoculated subcutaneously between the scapulae with varying doses of bacteria per mouse (as noted in Figure legends) in 100 μl. For i.v. ID_{50} determinations, mice were inoculated retro-orbitally with varying doses of bacteria per mouse in 100 μl. In each experiment, control mice were sham inoculated with 100 μl PBS + 0.2% NMS. Two or 4 weeks post-inoculation, mice were euthanized by CO_2 narcosis and tissues including the heart, tibiotarsal joint, inoculation site skin (or skin between the scapulae in i.v. ID_{50} experiments) and ear were harvested for culture and for quantification of bacterial load by qPCR. Cultures were checked for the presence of *B. burgdorferi* by dark-field microscopy for up to 8 weeks after which a final designation of positive or negative was assigned. ID_{50} values were calculated from the infection status of each mouse based on culture results. A mouse was designated as infected if any culture was positive.

Quantitative PCR

Bacterial burdens were quantified as described (Ristow *et al*., 2012). Briefly, DNA was harvested from tissue samples using the

QIAGEN QIAamp DNA Mini Kit. The *B. burgdorferi* standard curve was generated in the presence of a constant amount of mouse DNA, using DNA isolated from *B. burgdorferi* grown in culture and mouse LA-4 cells (ATCC #CCL 196) or uninfected mouse livers using the same kit. The mouse standard curve was generated from DNA isolated from mouse LA-4 cells or uninfected mouse livers. Standards and samples were run in triplicate with primers to detect *recA* for quantification of *B. burgdorferi* or mouse β-actin for quantification of mouse genomic DNA on a BioRad CFX96 cycler. After generation of a standard curve with BioRad CFX Manager 3.0 software, the experimental value for each sample was extrapolated from the average Ct value for each triplicate and all values were increased by 1 to facilitate plotting on a log scale. Results are presented as the number of *B. burgdorferi* genomes per 10^4 mouse genomes for each sample. The limit of detection for *Borrelia* genomes was six genomes per reaction. The limit of detection for mouse genomes was three haploid genomes per reaction.

Construction and expression of MBP-P66 fusion proteins

The parental MBP-P66M fusion was previously described (Coburn *et al*., 1999) and includes the region of P66 required for integrin binding. Briefly, the pMalC2 vector (New England Biolabs) was utilized to generate a MBP fusion with the middle portion of P66, containing a.a. 170–404. To test the roles of specific amino acids in integrin binding of P66, mutations were generated within the coding sequence of the hypothesized integrin-binding region (Defoe and Coburn, 2001) of P66 using the Stratagene QuikChange II site-directed mutagenesis kit (Agilent Technologies) per manufacturer instructions. Primers were designed to generate two single amino acid changes (a.a. D205A and D207A) or to delete a portion of P66 (a.a. 202–208). Primer sequences are described in Supporting Information Table S3. Mutagenized vectors were transformed into *E. coli* BLR and transformants were plated on LB plates with 0.2% dextrose and 100 μg ml^{-1} ampicillin for selection. Six clones from each intended mutation were purified by restreaking. Clones confirmed by sequencing to contain the targeted mutations were transformed into *E. coli* KS330 for optimal protein expression, and are referred to as P66M-D205A,D207A or P66M-Del202–208. Protein expression was induced with IPTG (isopropyl β-D-1-thiogalactopyranoside). Cells were lysed by French Press and proteins were purified by amylose affinity chromatography as described previously (Leong *et al*., 1990; Coburn *et al*., 1999). MBP-β-gal (encoded by the vector) was used as a control for background binding of MBP-fusion proteins. Protein concentration was quantified using the Bradford Assay (Bio-Rad) before use in assays.

Construction of B. burgdorferi *strains*

Construction of HB19 *Δp66* (HB19/K04) was previously described (Coburn and Cugini, 2003). Complementation of this strain was performed using the previously described construct, pBSV2G*p66* (Ristow *et al*., 2012). Successful transformation of this construct into *B. burgdorferi* results in P66 expression from the autonomously maintained shuttle vector. Targeted mutations of P66 at a.a. 205 and 207 or deletion of a.a. 202–208 were generated as described for the MBP-P66 fusions using pBSV2G*p66* as a template. Clones were isolated after transformation of these constructs into HB19 *Δp66* and screened by PCR for the presence of appropriate drug resistance markers. Restoration of P66 expression was observed by immunoblot using anti-P66 rabbit antiserum (Coburn and Cugini, 2003) as the primary antibody. Anti-rabbit IgG-alkaline phosphatase conjugate (Promega) was used as the secondary antibody for colorimetric visualization of P66 expression. Retention of plasmids found in the parental strain was monitored by PCR using two different primer sets for each clone as previously described (Elias *et al*., 2002; Bunikis *et al*., 2011). Clones with restoration of P66 expression, mutations confirmed by sequencing, and retention of the parental genomic content were used in this study and are referred to as $p66^{cp}$ (complement on the plasmid), *HD205A,D207A* or *HDel202–208*. These strains were indistinguishable from the WT strain in *in vitro* growth and were used to quantify binding to mammalian cells.

Construction of B31 A3 *Δp66* and $p66^{cc}$ (complement on the chromosome) strains was previously described (Ristow *et al*., 2012). Targeted mutations within P66 were generated to be expressed in the infectious strain background, B31 A3 (Elias *et al*., 2002), in the same manner as MBP-P66 described above, using pGTE*p66* (Ristow *et al*., 2012) as a template. Upon transformation into *B. burgdorferi*, pGTE*p66* allows homologous recombination of the *p66* coding region and flanking sequences into the endogenous locus on the chromosome to restore P66 expression to a *Δp66* strain. Transformation with the linearized construct resulted in candidate *B. burgdorferi* clones that were screened as described above for HB19 strains. Clones with restoration of P66 expression, mutations confirmed by sequencing and retention of the complete parental genome were used in the work reported here and are referred to as *BD205A,D207A* or *BDel202–208*. These strains were indistinguishable from the WT strain in *in vitro* growth and were used in transmigration assays, ID_{50} determinations and quantification of bacterial burdens in different tissue sites.

Analysis of surface expression of P66

Bacteria from 3 ml of growing cultures (1–5 × 10^7 bacteria ml^{-1}) of HB19 or B31 A3 strains and derivatives were subjected to centrifugation for 30 min at 1500 × g at ambient temperature (room temperature, RT). After removal of supernatant fluid, bacteria were suspended in 1 ml of PBS and subjected to centrifugation for 8 min at 11 200 × g at RT. After removal of supernatant fluid, bacteria were suspended in 1 ml of PBS and split into four tubes. Bacteria were incubated with varying concentrations of proteinase K (0, 1, 10 and 100 μg ml^{-1}) for 1 h at 33°C. After proteinase K treatment, phenylmethylsulfonyl fluoride was added to a final concentration of 0.2 mM for 15 min at RT. Cultures were subjected to centrifugation for 8 min at 11 200 × g and pelleted bacteria were suspended in PBS to a final concentration of 5 × 10^9 bacteria per ml. An equal volume of 2 × sample buffer with β-mercaptoethanol was added before boiling samples at 100°C for 5 min. Ten microlitres of each sample was fractionated by SDS-PAGE (10% acrylamide), transferred to Immobilon, and probed with rabbit anti-P66 (1:5000 dilution) and mouse anti-flagellin H9724 (1:500 dilution) (provided by Dr Tom Schwan) as a loading control and for assessment of outer membrane integrity. Goat anti-rabbit IgG-alkaline phosphatase conjugate (1:10 000 dilution) and goat anti-mouse IgG-alkaline

phosphatase conjugate (1:10 000 dilution) (Promega) were used as secondary antibodies and colorimetric methods were used to visualize bands.

Mammalian cell culture

Human embryonic kidney cell line 293 (HEK293) stably expressing human integrin $\alpha_v\beta_3$ (293 + $\alpha_v\beta_3$) (LaFrance *et al.*, 2011) was cultured in Dulbecco's modified Eagle medium plus Ham's F12 nutrient mix (base medium; Gibco) with 5% heat-inactivated fetal bovine serum (FBS) (Gibco) supplemented with 400 μg ml^{-1} of G418 (Gibco). Human microvascular endothelial cells (HMEC-1) (Ades *et al.*, 1992) were cultured in MCDB 131 (base medium; Gibco) with 15% heat-inactivated Hyclone FBS (Hyclone Laboratories), 1 μg ml^{-1} of hydrocortisone (Sigma-Aldrich), 10 ng ml^{-1} of epidermal growth factor (Gibco) and 25 mM HEPES (Gibco). The mouse lung epithelial cell line LA-4 was cultured in Kaighn's modification of Ham's F12 medium (F12K) (base medium; Gibco) with 10% heat-inactivated FBS (Gibco) (Stoner *et al.*, 1975). All cell lines were cultured in the presence of additional L-glutamine (Gibco) to a final concentration of 2 mM and for general maintenance of cell lines, penicillin at a concentration of 100 U ml^{-1} and streptomycin to a final concentration of 100 μg ml^{-1} (Gibco). For bacterial infections, antibiotic containing medium was removed and cells were washed before being lifted with Trypsin-EDTA (Gibco) and suspended in antibiotic free medium prior to being plated in the absence of antibiotics. Cells were incubated at 37°C under 5% CO_2.

Assessment of P66 binding to purified integrin $\alpha_v\beta_3$

Purified recombinant mouse and human integrin $\alpha_v\beta_3$ (carrier free) were purchased from R&D Systems. Purified MBP fusions to P66M (WT), D205A,D207A, Del202–208 and β-galactosidase (β-gal) were diluted to concentrations indicated in HEPES-buffered saline with cations (HBSC; 25 mM HEPES, 150 mM NaCl, 1 mM $MgCl_2$, 1 mM $MnCl_2$, 0.25 mM $CaCl_2$). Interactions of P66 with mouse or human integrin $\alpha_v\beta_3$ were analysed by SPR using a Biacore 3000 (GE Healthcare). Ten μg of MBP-P66M, MBP-D205A,D207A, or MBP-Del202–208, or MBP-βgal (negative control) was conjugated to an CM5 chip (GE Healthcare). A control flow cell was injected with HBSC buffer without mouse or human integrin $\alpha_v\beta_3$. For quantitative SPR experiments to determine integrin $\alpha_v\beta_3$ binding, 20 μl of increasing concentrations (0, 31.25, 62.5, 125, 250, 500 nM) of a mouse or human integrin $\alpha_v\beta_3$ were injected into the control cell and flow cells with immobilized MBP-P66M, MBP-D205A,D207A, MBP-Del202–208, or MBP-βgal at 10 μl min^{-1}, 25°C. To obtain the kinetic parameters of the interaction, sensogram data were fitted by means of BIAevaluation software version 3.0 (GE Healthcare) using the one-step biomolecular association reaction model (1:1 Langmuir model), resulting in optimum mathematical fit with the lowest chi values.

Mammalian cell-binding assays

Confluent monolayers of 293 + $\alpha_v\beta_3$ cells were used in binding assays. Cells were cultured in sterile 96-well tissue culture plates 2 days prior to probing with purified recombinant protein. On the day of the assay, cell monolayers were washed once with PBS before the addition of base cell medium supplemented with 1% bovine serum albumin (BSA) (blocking buffer). Plates were blocked at 37°C for 1 h. Proteins were diluted in blocking buffer to 0.1 μM. Blocking buffer was removed and replaced with the test proteins and incubated at 37°C for 1 h. Wells were washed twice with PBS to remove unbound protein before fixing bound protein with 3% paraformaldehyde for 30 min or overnight. The plates were washed three times with Tris-buffered saline (TBS) to remove fixative, then blocked with TBS + 3% normal goat serum (NGS) + 1% BSA for 1 h. An ELISA was performed to assess bound protein using rabbit anti-MBP (1:10 000 dilution) in TBS + 3% NGS + 1% BSA as primary antibody, and goat anti-rabbit horseradish peroxidase (HRP) conjugate (1:10 000 dilution) in TBS + 3% NGS + 1% BSA as secondary antibody. Plates were developed using tetramethylbenzidine substrate tablets (Sigma-Aldrich) with hydrogen peroxide in a 1:10 mixture of dimethyl sulfoxide (DMSO) and 0.05 M phosphate-citrate buffer, pH 5.0. Colorimetric development was read by absorbance at 655 nm. After washing away developer, cell retention was measured with crystal violet, read at 595 nm. The ELISA signal was normalized to cell retention for individual wells, with quadruplicate measurements on each plate. Binding of mutant proteins was normalized to binding of MBP-P66M to allow incorporation of data from multiple experiments into the statistical analyses and figures, as raw optical density (OD) values were not always identical in different experiments. Statistical analyses were performed using one-way ANOVA with Dunn's multiple comparison post-test in GraphPad Prism version 5.1.

For assessment of binding of *B. burgdorferi* strain HB19-derived bacteria, the protocol was similar. On the day of the assay, after blocking, cell monolayers were washed and probed with 50 μl of bacteria at 2.5×10^7 bacteria per ml for 1 h at 37°C. Unbound bacteria were washed away and bound bacteria were fixed in 3% paraformaldehyde for 30 min or overnight. The plates were washed three times with TBS to remove fixative, then blocked with TBS + 3% NGS + 1% BSA for 1 h. An ELISA was performed using rabbit anti-Lyme spirochete serum (1:10 000 dilution) (provided by Dr Allen Steere) in TBS + 3% NGS + 1% BSA as primary antibody, followed by goat anti-rabbit HRP conjugate (1:10 000 dilution) in TBS + 3% NGS + 1% BSA as secondary antibody. Plates were developed and ELISA signal was normalized to cell retention as described for MBP-fusion proteins. Binding of bacteria expressing mutant P66 proteins was normalized to binding of WT bacteria to allow incorporation of data from multiple experiments into the statistical analyses and figures, as raw OD values were not always identical in different experiments. Statistical analyses were performed using one-way ANOVA with Dunn's multiple comparison post-test in GraphPad Prism version 5.1.

In vitro *transmigration*

HMEC-1 cells were plated onto 3 μm pore size Transwell inserts (Costar #3472 polyester membrane Transwell inserts) in growth medium without antibiotics, as previously described (Martinez-Lopez *et al.*, 2010). Endothelial cell monolayers were allowed to reach confluence over 72 h before infection with *B. burgdorferi* at an MOI of 20. The percentage of bacteria crossing into the chamber below was monitored over 72 h by removing aliquots from both top and bottom chambers and enumerating the bacteria in a Petroff-Hausser counting chamber using dark-field microscopy. Raw numbers of spirochetes were comparable between strains throughout the time course, with all strains

replicating through the 48 h time point. Beyond 48 h, bacterial health and numbers began to diminish and data were not reproducible. In parallel, FITC-Dextran 40 000 Da was added to an insert to assess confluence of the plated monolayers. Inserts without cells plated were used as controls for crossing of the membrane alone. Assays were performed in triplicate. Statistical analyses were performed using two-way ANOVA with Bonferroni's post-test in GraphPad Prism version 5.1.

Pore formation assay

Cultures of HB19 strains were grown until mid-late logarithmic phase and outer membrane proteins were purified as previously described (Magnarelli *et al*., 1989). Further purification of P66 was performed by anion exchange chromatography using a HiPrep Q XL 16/10 column (GE Healthcare). The method for black lipid bilayer experiments has been described previously (Benz *et al*., 1978). The bilayer equipment consists of a Teflon chamber with two compartments, separated by a thin wall with a small circular hole (0.4 mm^2) that connects the two compartments. Over the small hole, an artificial bilayer membrane can be painted, into which proteins with channel-forming capabilities can insert. Insertion of pore-forming proteins causes a change in the membrane current that can be measured and used to calculate the size of the channel formed. The membrane solution was formed from 1% (w v^{-1}) diphytanoyl phosphatidylcholine (Avanti Polar Lipids) in n-decane. The protein containing solution was diluted 1:1 in 1% Genapol and added to the electrolyte on both sides when the membrane turned black. The two compartments contained 1 M KCl salt solution and the voltage applied was 20 mV. Membrane current was measured with a pair of Ag/AgCl electrodes with salt bridges switched in series with a voltage source and a current amplifier (Keithley 427). All experiments were performed at RT.

Acknowledgements

We thank Dr Dara Frank for providing access to her fluorescence microscope, Drs Yi-Guang Chen, Calvin Williams and Dipica Haribhai for their expertise and training in the diphtheria toxin receptor mouse model, Tarrant Csida and Jennifer Ritchie for performing intravenous mouse inoculations, Dr Allen Steere and Dr Tom Schwan for providing antibodies, the Ragon Institute Imaging Core Facility for providing access to SPR instrumentation, Michael Waring of the Imaging Core for assistance with SPR, and the staff in the Children's Hospital histology core for sectioning and staining mouse skin samples. This work was supported by NIH grants (R01-AI084873 and R01-AI093104), by the Swedish Research Council grant (07922), and by generous gifts from the MACC Fund and John B. and Judith A. Gardetto.

References

Ades, E.W., Candal, F.J., Swerlick, R.A., George, V.G., Summers, S., Bosse, D.C., and Lawley, T.J. (1992) HMEC-1: establishment of an immortalized human microvascular endothelial cell line. *J Invest Dermatol* **99:** 683–690.

Bárcena-Uribarri, I., Thein, M., Sacher, A., Bunikis, I., Bonde, M., Bergström, S., and Benz, R. (2010) P66 porins are present in both Lyme disease and relapsing fever spirochetes: a comparison of the biophysical properties of P66 porins from six *Borrelia* species. *Biochim Biophys Acta* **1798:** 1197–1203.

Bagos, P.G., Liakopoulos, T.D., Spyropoulos, I.C., and Hamodrakas, S.J. (2004) PRED-TMBB: a web server for predicting the topology of beta-barrel outer membrane proteins. *Nucleic Acids Res* **32:** W400–W404.

Barbour, A.G., Burgdorfer, W., Grunwaldt, E., and Steere, A.C. (1983) Antibodies of patients with Lyme disease to components of the *Ixodes dammini* spirochete. *J Clin Invest* **72:** 504–515.

Barczyk, M., Carracedo, S., and Gullberg, D. (2010) Integrins. *Cell Tissue Res* **339:** 269–280.

Behera, A.K., Durand, E., Cugini, C., Antonara, S., Bourassa, L., Hildebrand, E., *et al*. (2008) *Borrelia burgdorferi* BBB07 interaction with integrin alpha3beta1 stimulates production of pro-inflammatory mediators in primary human chondrocytes. *Cell Microbiol* **10:** 320–331.

Benz, R., Janko, K., Boos, W., and Läuger, P. (1978) Formation of large, ion-permeable membrane channels by the matrix protein (porin) of *Escherichia coli*. *Biochim Biophys Acta* **511:** 305–319.

Boyden, S. (1962) The chemotactic effect of mixtures of antibody and antigen on polymorphonuclear leucocytes. *J Exp Med* **115:** 453–466.

Bunikis, I., Kutschan-Bunikis, S., Bonde, M., and Bergström, S. (2011) Multiplex PCR as a tool for validating plasmid content of *Borrelia burgdorferi*. *J Microbiol Methods* **86:** 243–247.

Coburn, J., and Cugini, C. (2003) Targeted mutation of the outer membrane protein P66 disrupts attachment of the Lyme disease agent, *Borrelia burgdorferi*, to integrin alphavbeta3. *Proc Natl Acad Sci USA* **100:** 7301–7306.

Coburn, J., Leong, J.M., and Erban, J.K. (1993) Integrin alpha IIb beta 3 mediates binding of the Lyme disease agent *Borrelia burgdorferi* to human platelets. *Proc Natl Acad Sci USA* **90:** 7059–7063.

Coburn, J., Barthold, S.W., and Leong, J.M. (1994) Diverse Lyme disease spirochetes bind integrin alpha IIb beta 3 on human platelets. *Infect Immun* **62:** 5559–5567.

Coburn, J., Magoun, L., Bodary, S.C., and Leong, J.M. (1998) Integrins alpha(v)beta3 and alpha5beta1 mediate attachment of lyme disease spirochetes to human cells. *Infect Immun* **66:** 1946–1952.

Coburn, J., Chege, W., Magoun, L., Bodary, S.C., and Leong, J.M. (1999) Characterization of a candidate *Borrelia burgdorferi* beta3-chain integrin ligand identified using a phage display library. *Mol Microbiol* **34:** 926–940.

Cugini, C., Medrano, M., Schwan, T.G., and Coburn, J. (2003) Regulation of expression of the *Borrelia burgdorferi* beta(3)-chain integrin ligand, P66, in ticks and in culture. *Infect Immun* **71:** 1001–1007.

Defoe, G., and Coburn, J. (2001) Delineation of *Borrelia burgdorferi p66* sequences required for integrin alpha(IIb)beta(3) recognition. *Infect Immun* **69:** 3455–3459.

Elias, A.F., Stewart, P.E., Grimm, D., Caimano, M.J., Eggers, C.H., Tilly, K., *et al*. (2002) Clonal polymorphism of *Borrelia burgdorferi* strain B31 MI: implications for mutagenesis in

an infectious strain background. *Infect Immun* **70:** 2139–2150.
Herter, J., and Zarbock, A. (2013) Integrin regulation during leukocyte recruitment. *J Immunol* **190:** 4451–4457.
Hodivala-Dilke, K.M., McHugh, K.P., Tsakiris, D.A., Rayburn, H., Crowley, D., Ullman-Culleré, M., *et al*. (1999) Beta3-integrin-deficient mice are a model for Glanzmann thrombasthenia showing placental defects and reduced survival. *J Clin Invest* **103:** 229–238.
Kenedy, M.R., Luthra, A., Anand, A., Dunn, J.P., Radolf, J.D., and Akins, D.R. (2014) Structural modeling and physicochemical characterization provide evidence that P66 forms a beta-barrel in the *Borrelia burgdorferi* outer membrane. *J Bacteriol* **196:** 859–872.
LaFrance, M.E., Pierce, J.V., Antonara, S., and Coburn, J. (2011) The *Borrelia burgdorferi* integrin ligand P66 affects gene expression by human cells in culture. *Infect Immun* **79:** 3249–3261.
Leong, J.M., Fournier, R.S., and Isberg, R.R. (1990) Identification of the integrin binding domain of the *Yersinia pseudotuberculosis* invasin protein. *EMBO J* **9:** 1979–1989.
Leong, J.M., Morrissey, P.E., Marra, A., and Isberg, R.R. (1995) An aspartate residue of the *Yersinia pseudotuberculosis* invasin protein that is critical for integrin binding. *EMBO J* **14:** 422–431.
Magnarelli, L.A., Anderson, J.F., and Barbour, A.G. (1989) Enzyme-linked immunosorbent assays for Lyme disease: reactivity of subunits of *Borrelia burgdorferi*. *J Infect Dis* **159:** 43–49.
Martinez-Lopez, D.G., Fahey, M., and Coburn, J. (2010) Responses of human endothelial cells to pathogenic and non-pathogenic *Leptospira* species. *PLoS Negl Trop Dis* **4:** e918.
Moriarty, T.J., Norman, M.U., Colarusso, P., Bankhead, T., Kubes, P., and Chaconas, G. (2008) Real-time high resolution 3D imaging of the Lyme disease spirochete adhering to and escaping from the vasculature of a living host. *PLoS Pathog* **4:** e1000090.
Moriarty, T.J., Shi, M., Lin, Y.P., Ebady, R., Zhou, H., Odisho, T., *et al*. (2012) Vascular binding of a pathogen under shear force through mechanistically distinct sequential interactions with host macromolecules. *Mol Microbiol* **86:** 1116–1131.
Norman, M.U., Moriarty, T.J., Dresser, A.R., Millen, B., Kubes, P., and Chaconas, G. (2008) Molecular mechanisms involved in vascular interactions of the Lyme disease pathogen in a living host. *PLoS Pathog* **4:** e1000169.
Orlando, R.A., and Cheresh, D.A. (1991) Arginine-glycine-aspartic acid binding leading to molecular stabilization between integrin alpha v beta 3 and its ligand. *J Biol Chem* **266:** 19543–19550.
Pinne, M., Thein, M., Denker, K., Benz, R., Coburn, J., and Bergström, S. (2007) Elimination of channel-forming activity by insertional inactivation of the *p66* gene in *Borrelia burgdorferi*. *FEMS Microbiol Lett* **266:** 241–249.
Preac-Mursic, V., Wilske, B., and Schierz, G. (1986) European *Borrelia burgdorferi* isolated from humans and ticks culture conditions and antibiotic susceptibility. *Zentralbl Bakteriol Mikrobiol Hyg A* **263:** 112–118.
Reed, L.J., and Muench, H. (1938) A simple method of estimating fifty per cent endpoints. *Am J Epidemiol* **27:** 493–497.
Ristow, L.C., Miller, H.E., Padmore, L.J., Chettri, R., Salzman, N., Caimano, M.J., *et al*. (2012) The beta(3)-integrin ligand of *Borrelia burgdorferi* is critical for infection of mice but not ticks. *Mol Microbiol* **85:** 1105–1118.
Samuels, D.S. (1995) Electrotransformation of the spirochete *Borrelia burgdorferi*. *Methods Mol Biol* **47:** 253–259.
Skare, J.T., Mirzabekov, T.A., Shang, E.S., Blanco, D.R., Erdjument-Bromage, H., Bunikis, J., *et al*. (1997) The Oms66 (*p66*) protein is a *Borrelia burgdorferi* porin. *Infect Immun* **65:** 3654–3661.
Springer, T.A. (1994) Traffic signals for lymphocyte recirculation and leukocyte emigration: the multistep paradigm. *Cell* **76:** 301–314.
Stephens, L.E., Sutherland, A.E., Klimanskaya, I.V., Andrieux, A., Meneses, J., Pedersen, R.A., and Damsky, C.H. (1995) Deletion of beta 1 integrins in mice results in inner cell mass failure and peri-implantation lethality. *Genes Dev* **9:** 1883–1895.
Stoner, G.D., Kikkawa, Y., Kniazeff, A.J., Miyai, K., and Wagner, R.M. (1975) Clonal isolation of epithelial cells from mouse lung adenoma. *Cancer Res* **35:** 2177–2185.
Szczepanski, A., Furie, M.B., Benach, J.L., Lane, B.P., and Fleit, H.B. (1990) Interaction between *Borrelia burgdorferi* and endothelium *in vitro*. *J Clin Invest* **85:** 1637–1647.
Tran van Nhieu, G.T., and Isberg, R.R. (1991) The *Yersinia pseudotuberculosis* invasin protein and human fibronectin bind to mutually exclusive sites on the alpha 5 beta 1 integrin receptor. *J Biol Chem* **266:** 24367–24375.

Supporting information

Additional Supporting Information may be found in the online version of this article at the publisher's web-site:

Fig. S1. Wild-type and *Δp66 Borrelia burgdorferi* bacterial burdens are unaltered in $\beta_3^{-/-}$ mice compared with $\beta_3^{+/+}$ mice. $\beta_3^{+/+}$ (filled symbols) or $\beta_3^{-/-}$ (open symbols) mice were inoculated with B31-A3 (wild-type) (squares) or *Δp66* (triangles) *B. burgdorferi* at a range of doses (10^3–10^9). Tissues were harvested 4 weeks post-inoculation and total DNA was purified and analyzed by qPCR with primers to detect *Borrelia* genomes or mouse genomes. Bacterial loads in mice inoculated at 10^5 are shown. Mean bacterial load is indicated with error bars representing standard deviation. Statistical analyses were performed using a two-way ANOVA with Bonferroni's post-test. $^*P < 0.05$, $^{**}P < 0.01$, $^{***}P < 0.001$. $n = 5$ mice per group.

Fig. S2. Mutation of *p66* does not increase sensitivity to complement. (A) *B. burgdorferi* strains in the B31-A3 background were incubated with 40% complete or 40% heat-inactivated (HI) human serum in triplicate. Aliquots from each condition were plated in solid BSK II at 1, 2, 4 and 16 h, incubated at 33°C for 2 weeks and colonies were enumerated. The mean concentration of viable bacteria per millilitre is indicated with error bars representing standard error. $n = 3$. (B) *E. coli* MC1061 bacteria were incubated with no serum, 40% complete or 40% heat-inactivated (HI) human serum in triplicate. A dilution series from each condition was plated on LB agar at 1, 2, 4 and 16 h, incubated at 37°C for 16 h and colonies were enumerated. The mean concen-

tration of viable bacteria per millilitre is indicated with error bars representing standard error. $n = 3$.

Fig. S3. Depletion of macrophages or dendritic cells does not affect infection by either wild-type or *Δp66 B. burgdorferi*. (A and B) The site of inoculation was harvested at days 1, 2, 3, 4, 5, 6 and 8 from transgenic mice expressing diphtheria toxin receptor (DTxR) on macrophages inoculated with either B31-A3 (wild-type) or *Δp66* bacteria plus diphtheria toxin (DTx) or the enzymatically inactive cross-reactive mutant form of the toxin (CRM) (A), or from C57Bl/6 mice inoculated with wild-type or *Δp66* bacteria with no toxin (B). Sham-inoculated mice were used as controls on days 1 and 8 (B). Note that DTx-treated mice were euthanized and tissues harvested as the mice began to show signs of illness, so CRM-treated mice and C57Bl/6 mice were not always euthanized and harvested for the same time points. (C and D) The site of inoculation was harvested at days 1, 2, 4 and 5 from transgenic mice expressing DTxR on dendritic cells inoculated with either B31-A3 (wild-type) or *Δp66* bacteria plus DTx or CRM (C), or from C57Bl/6 mice inoculated with wild-type or *Δp66* bacteria with no toxin (D). Sham-inoculated mice were used as controls on days 1 and 5 (D). DNA was purified from the tissue and analysed by qPCR with primers to detect *Borrelia* DNA or mouse DNA. Statistical analyses were performed between groups of mice on each day of harvest using one-way ANOVA Kruskal–Wallis test with Dunn's multiple comparison post-test. $^{*}P < 0.05$, $^{**}P < 0.01$. Mean bacterial load is indicated with error bars representing standard deviation. $n = 5$ mice per condition.

Fig. S4. Depletion of macrophages or dendritic cells in DTxR transgenic mice treated with DTx. Top row: immunohistochemical staining of anti-F4/80-reactive cells in inoculation site skin of mice treated with CRM (left panel) or DTx (right panel) at day 1 post-inoculation and intoxication. Scale bars = 20 μm; images acquired at 100× magnification. Bottom row: fluorescence imaging of the site of inoculation at day 1 post-inoculation and intoxication with B31-A3 (wild-type) *B. burgdorferi* expressing tdTomato (red) and CRM (left panel) or DTx (right panel). Dendritic cells in this transgenic mouse model express DTxR and eGFP (green). Spirochetes are indicated with an arrow. Scale bars = 20 μm; images acquired at 200× magnification.

Table S1. Subcutaneous ID_{50} determinations of B31-A3 (wild-type) and *Δp66 Borrelia burgdorferi* in $\beta_3^{+/+}$ or $\beta_3^{-/-}$ mice 4 weeks post-inoculation.

Table S2. Bacterial strains and plasmids used in this study.

Table S3. Oligonucleotide primers, 5′ → 3′.

Video S1. Motility of wild-type and *Δp66 B. burgdorferi* is similar at the site of inoculation *in vivo*. RFP expressing B31 A3 and GFP expressing *Δp66 B. burgdorferi* were imaged at the site of inoculation 1 h post-intradermal inoculation. A time-lapse video was acquired at a magnification of 20×, exposure time of 2 s for each colour (green and red), time lapse set at 2 s interval for 5 min. For movie conversion, output timing was set at the interval of 200 ms.

Appendix S1. Supplemental experimental procedures.

Appendix S2. Supplemental experiments.